

IMECE2004-60065

A FEEDBACK CONTROLLED CARBON NANOTUBE BASED NEMS DEVICE: CONCEPT AND MODELING

Changhong Ke and Horacio D. Espinosa*
Department of Mechanical Engineering, Northwestern University
Evanston, IL 60208-3111, USA

* Author to whom correspondence should be addressed; E-mail: espinosa@northwestern.edu.

ABSTRACT

A switchable carbon nanotube based nano-electromechanical systems (NEMS) device with close-loop feedback is examined. The device is made of a conductive multi-walled carbon nanotube (MWNT) placed as a cantilever over a micro-fabricated step. A bottom electrode, power supply and a resistor are also parts of the device circuit. The pull-in/pull-out and tunneling characteristics of the device are investigated by means of an electro-mechanical analysis. The model includes the concentration of electrical charge, at the end of the nanocantilever, and the *van der Waals* force. Finite kinematics accounting for large deformations of the cantilever is also included in the modeling. The result shows that the device has two well-defined stable equilibrium positions as a result of the tunneling and the incorporation of a feedback resistor to the circuit. The potential applications of the device include NEMS switches, random-access memory (RAM) elements, logic devices and electron-counters.

INTRODUCTION

Nanoelectromechanical systems (NEMS) are attracting significant attention because of their properties to enable superior electronic components and sensors. By exploiting nanoscale effects, NEMS present interesting and unique characteristics. For instance, NEMS based devices can have an extremely high fundamental frequency,¹⁻⁴ and preserve very high mechanical responsivity.⁵ Several NEMS devices have been reported, such as mass sensors,⁶ RF resonators,⁶ FETs⁷ and electrometers.⁸ Carbon nanotubes (CNTs) have long been considered ideal building blocks for NEMS devices due to their distinguished electrical and mechanical properties. CNT-based NEMS devices reported in literature include nanotweezers,⁹⁻¹⁰

nonvolatile random access memory (RAM),¹¹ nanorelays¹² and rotational actuators.¹³

In this paper, a CNT-based NEMS device with feedback control is investigated. The device, schematically shown in Fig.1, is made of a conductive multi-walled carbon nanotube (MWNT) placed as a cantilever over a micro-fabricated step. A bottom electrode, a resistor and a power supply are parts of the device circuit. When the applied voltage $U < V_{PI}$ (*pull-in* voltage), the electrostatic force is balanced by the elastic force from the deflection of the CNT cantilever. The CNT cantilever remains in the “upper” equilibrium position. The deflection is controlled by the applied voltage. When the applied voltage exceeds a *pull-in* voltage, the system becomes unstable. With any increase in the applied voltage U , the electrostatic force becomes larger than the elastic force and the CNT accelerates towards the bottom electrode. When the tip of the CNT is very close to the electrode (i.e., gap $\Delta \approx 0.7$ nm) as shown in Fig.1, substantial tunneling current passes between the tip of the CNT and the bottom electrode. Due to the existence of the resistor R in the circuit, the voltage applied to the CNT drops, weakening the electric field. Because of the kinetic energy of the CNT, it continues to deflect downward and the tunneling current increases, weakening the electric field further. In this case, the elastic force is larger than the electrostatic force and the CNT decelerates and changes the direction of motion. This decreases the tunneling current and the electrical field recovers. If there is damping in the system, the kinetic energy of the CNT is dissipated and the CNT stays at the position where the electrostatic force is equal to the elastic force and a stable tunneling current is established in the device. This is the “lower” equilibrium position for the CNT cantilever. At this point, if the applied voltage U decreases, the CNT cantilever starts retracting. When U decreases to a certain value, called

pull-out voltage V_{PO} , the CNT cantilever is released from its lower equilibrium position and returns back to its upper equilibrium position. At the same time, the current in the device diminishes substantially. Basically the *pull-in* and *pull-out* processes follow a hysteric loop for the applied voltage and the current in the device. The upper and lower equilibrium positions correspond to “ON” and “OFF” states of a switch, respectively. Also the existence of the tunneling current and feedback resistor make the “lower” equilibrium states very robust, which is key to some applications of interest.

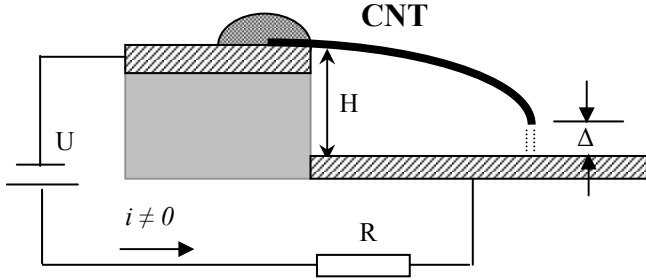


Figure 1. Schematic of CNT based device with tunneling contacts. H is the initial step height and Δ is the gap between the deflected tip and bottom conductive substrate. R is the feedback resistor.

MODELING

A quantification of the phenomenon previously described is made here by means of electro-mechanical modeling of the device. The carbon nanotube considered here is a homogeneous, perfect conductor of length L , with outer and inner radii R_{ext} and R_{int} , respectively. When the cylinder is biased with the substrate grounded, clearly there are distributed charges along the side surface of the cylinder and concentrated charges around the ends. The charge distribution along a carbon nanotube with finite length has been investigated by full 3D numerical simulation using CFD-ACE+ (a commercial code from CFD Research Corporation).

Figure 2 shows the charge distribution along the length of a free standing carbon nanotube subjected to a biased voltage of 1 volt. The contour plot shows the charge density (side view), while the curve shows the charge per unit length along the cylinder. For a one-end-clamped cylinder beam, as is the case for the device under examination, the capacitance per unit length along the nanotube can be approximated as¹⁴

$$C = C_d(r) \left\{ 1 + 0.85 \left[(H + R_{ext})^2 R_{ext} \right]^{1/3} \delta(z - L) \right\} \\ = C_d(r) (1 + f_c) \quad (1)$$

where the first term in the bracket accounts for the uniform charge along the side surface of the tube and the second term, f_c , accounts for the concentrated charge at the end of the tube. $\delta(z)$ is the Dirac distribution function and z is the axial coordinate of the nanotube.

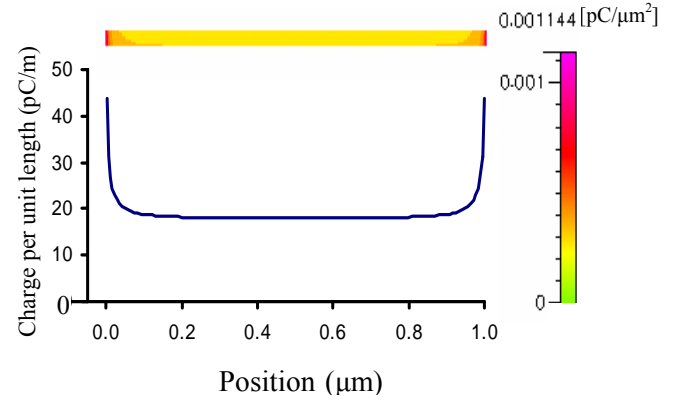


Figure 2. Charge distribution for a biased nanotube. The parameters are $R_{ext}=9\text{nm}$, $H=100\text{nm}$ and $L=1\mu\text{m}$.

$C_d(r)$ is the distributed capacitance along the side surface per unit length for an infinitely long tube, which is given by¹⁵

$$C_d(r) = \frac{2\pi\epsilon_0}{\cosh^{-1}(r/R_{ext})} \quad (2)$$

where r is the distance between the axis of the cylinder and the substrate, and ϵ_0 is the permittivity of vacuum ($\epsilon_0 = 8.854 \times 10^{-12} \text{C}^2\text{N}^{-1}\text{m}^{-2}$).

Considering the cantilever under small deformation, the electrostatic force per unit length is given by

$$q_{elec} = \frac{1}{2} V^2 \left(\frac{dC_d}{dr} \right) \{1 + f_c\} \quad (3)$$

The *upper equilibrium* equation for the CNT cantilever, based on a continuum model, is given by,

$$EI \frac{d^4 w}{dz^4} = q_{elec} + q_{vdw} \quad (4)$$

where E is the CNT Young's modulus and w is the deflection. I is the moment of inertia of the nanotube cross-section, i.e., $I = \pi(R_{ext}^4 - R_{int}^4)/4$. q_{vdw} is the *van der Waals* force (per unit length) between the nanotube and the substrate and can be evaluated using the method reported originally by Reuckes et al.¹¹ and later employed by Dequesnes et al.,¹⁶ assuming that the substrate consists of 30 graphite layers.

For cantilever with large deformation, finite kinematics needs to be considered as the govern equation for equilibrium should be rewritten as

$$EI \frac{d^2}{dx^2} \left[\frac{\frac{d^2 w}{dx^2}}{\left[1 + \left(\frac{dw}{dx} \right)^2 \right]^{\frac{3}{2}}} \right] = (q_{\text{elec}} + q_{\text{vdw}}) \sqrt{1 + \left(\frac{dw}{dx} \right)^2} \quad (5)$$

where q_{elec} and q_{vdw} are the same as in Eq. (4).

Numerical integration of Eq. (4) or (5) provides the tip deflection, as a function of applied voltage, as well as the *pull-in* voltage.

In regard to the *pull-in* voltage, an analytically derived formula based on energy method has been reported recently, without considering the *van der Waal* force, as¹⁷

$$V_{\text{PI}} \approx k \sqrt{\frac{1+k^{\text{FK}}}{1+k^{\text{TIP}}}} \frac{H}{L^2} \ln \left(\frac{2H}{R_{\text{ext}}} \right) \sqrt{\frac{EI}{\epsilon_0}}$$

$$k \approx 0.85; k^{\text{FK}} \approx \frac{8H^2}{9L^2}; k^{\text{TIP}} \approx \frac{2.55(R_{\text{ext}}(H+R_{\text{ext}}))^{\frac{1}{3}}}{L} \quad (6)$$

Here superscript FK and TIP refer to finite kinematics and concentrated charge at the tip of nanotube, respectively. This analytical formula for *pull-in* voltage shows good agreement with the results by numerically solving Eq. (4) or (5), thus provides an efficient way to assess the *pull-in* voltage based on geometry of the device.

To examine the *lower equilibrium configuration*, the current flow in the system needs to be included. The resistance of the tunneling contact between the tip of the nanotube and the bottom electrode in the environment of vacuum can be described as $R_{\text{T}}[\Delta] = R_0 \exp(\Delta/\lambda)$.³ Here R_0 is the contact resistance between the nanotube and the bottom electrode and can be evaluated from experimental results.¹⁸ λ is a material

constant defined by $\lambda^{-1} = 1.02 \sqrt{\Phi(\text{eV})} \text{ \AA}^{-1}$, with Φ being the work function (for MWNT $\Phi \approx 5.0 \text{ eV}$).¹⁹ Hence, $\lambda^{-1} \approx 2.28 \text{ \AA}^{-1}$, which implies that the contact resistance increases by nearly one order of magnitude for every 1 \AA increase of the gap size.

When the gap between the free end of the carbon nanotube and the substrate becomes very small (e.g., $\Delta \approx 0.7 \text{ nm}$), a tunneling current is established in the device. Since in our approach the resistance of the carbon nanotube itself and the contact resistance between carbon nanotube and electrode are negligible compared with the feedback resistor in the circuit, so the potential along the carbon nanotube is considered to be constant here and the relation between the voltage drop V across the gap and the gap size Δ can be described as:

$$\frac{V}{U} \frac{R}{R_0} \exp(-\Delta/\lambda) = 1 - \frac{V}{U} \quad (7)$$

The corresponding tunneling current is $i = \frac{V}{R_0} \exp(-\Delta/\lambda)$.

From Eq. (7), we can see that the voltage drop across the gap, V , is not only dependent on gap size, but also dependent on the feedback resistance R .

By solving Eqs. (5) and (7) simultaneously, the voltage-gap relation for the “lower” equilibrium position is obtained.

RESULT AND DISCUSSION

In regard to the selection of the device geometry, we consider current available techniques for positioning carbon nanotubes, such as nanomanipulation,²⁰⁻²¹ CVD selective growth²² and DC/AC dielectrophoretic trapping.²³⁻²⁴ An initial step height H in the range of 100 nm ~ 1.5 μm seems realistic and consistent with demonstrated experimental techniques. For an examination of the device performance, we used the following parameters: multiwall CNT with $E = 1.2 \text{ TPa}$, $R_{\text{int}} = 6 \text{ nm}$ and 10 layers (intra-layer distance is assumed 0.335 nm), $L = 500 \text{ nm}$ and $H = 100 \text{ nm}$. Resistances $R_0 = 1 \text{ K}\Omega$ and $R = 1 \text{ G}\Omega$ are also employed. By numerically solving Eqs. (5) and (7) using integration method,²⁵ we identify a *pull-in* voltage $V_{\text{PI}} = 22.80 \text{ volts}$ and a *pull-out* voltage $V_{\text{PO}} = 2.77 \text{ volts}$. Fig. 3 shows the plots of the Δ - U and i - U characteristic signatures. It is clearly seen that there is a hysteresis loop on each of the two characteristic curves shown in Fig. 3, which describes the “lower” and “upper” equilibrium stable positions and the *pull-in* and *pull-out* processes. The hysteresis loop can be controlled by appropriate selection of geometric and electric parameters. This hysteretic behavior can be exploited to build NEMS switches or random access memory elements operating at GHz frequencies.

The simulation result shows that the *van der Waals* (*vdw*) force is important in the design and optimization of the device. As expected, the *vdw* force becomes substantial when the deflected tip almost touches the substrate. If the *vdw* force is large enough to balance the elastic force, “stiction” occurs, which means that the nanotube cantilever will be held at the “lower” stable equilibrium position. For example, for the device considered above, if the length of the nanotube increases to 1 μm , “stiction” will take place. For some applications, this effect could be desirable, while for others such as switches in memory elements, it should be avoided.

In order to assess the effect of thermal vibrations on the device performance, the vibration of the nanotube is approximated by the model reported by Treacy, et al.²⁶ According to this model, the CNT tip vibration amplitude is A

$$= \sqrt{0.4243 \frac{L^3 kT}{E(R_{\text{ext}}^4 - R_{\text{int}}^4)}}, \text{ where } k \text{ is Boltzmann's}$$

constant ($1.38 \times 10^{-23} \text{ J/K}$) and T is the temperature in degrees Kelvin. For the nanocantilever with the above-considered parameters, this equation gives a vibration amplitude of 1.86 \AA at room temperature (300K) and 0.2 \AA at 4.2 K. It is noted that the tunneling current will vary with temperature. However, the overall characteristics of the device will not change, i.e., the thermal effects can not switch the CNT cantilever from the “lower” equilibrium position to the “upper” equilibrium position or vice versa.

ACKNOWLEDGMENTS

The authors acknowledge the support from the FAA through Award No. DTFA03-01-C-00031 and the NSF through award No. CMS-0120866. Work was also supported in part by the Nanoscale Science and Engineering Initiative of the National Science Foundation under NSF Award Number EEC-0118025.

REFERENCES

- 1 Y. T. Yang, K. L. Ekinici, X. M. H. Huang, L. M. Schiavone, M. L. Roukes, C. A. Zorman, and M. Mehregany, *Appl. Phys. Lett.* **78**, 162 (2001).
- 2 A. N. Cleland and M. L. Roukes, *Appl. Phys. Lett.* **69**, 2653 (1996).
- 3 A. Erbe, R. H. Blick, A. Tilke, A. Kriele, and P. Kotthaus, *Appl. Phys. Lett.* **73**, 3751 (1998).
- 4 X. M. H. Huang, C. A. Zorman, M. Mehregany, and M. L. Roukes, *Nature* **421**, 496 (2003).
- 5 M. L. Roukes, "Nanoelectromechanical system," Technical Digest of the 2000 Solid-State Sensor and Actuator Workshop, 2000.
- 6 G. Abadal, Z. J. Davis, B. Helbo, X. Borriese, R. Ruiz, A. Boisen, F. Campabadal, J. Esteve, E. Figueras, F. Perez-Murano, and N. Barniol, *Nanotechnology* **12**, 100 (2001).
- 7 R. Martel, T. Schmidt, H. R. Shea, T. Hertel, and Ph. Avouris, *Appl. Phys. Lett.* **73**, 2447 (1998).
- 8 A. N. Cleland and M. L. Roukes, *Nature* **392**, 160 (1998).
- 9 S. Akita, Y. Nakayama, S. Mizooka, Y. Takano, T. Okawa, Y. Miyatake, S. Yamanaka, M. Tsuji, and T. Nosaka, *Appl. Phys. Lett.* **79**, 1691 (2001).
- 10 P. Kim and C. M. Lieber, *Science* **126**, 2148 (1999).
- 11 T. Rueckes, K. Kim, E. Joslevich, G. Y. Tseng, C. Cheung, and C. M. Lieber, *Science* **289**, 94 (2000).
- 12 J. Kinaret, T. Nord, and S. Viefers, *Appl. Phys. Lett.* **82**, 1287 (2002).
- 13 A. M. Fennimore, T. D. Yuzvinsky, W. Q. Han, M. S. Fuhrer, J. Cummings, and A. Zettl, *Nature* **424**, 408 (2003).
- 14 C. H. Ke, and H. D. Espinosa, "Analysis of electrostatic charge distribution in nanotubes and nanowires," submitted for publication to *J. Appl. Physics*, 2004.
- 15 W. Hayt and J. Buck, *Engineering Electromagnetics*, McGraw-Hill, 2001, 6th Edition.
- 16 M. Dequesnes, S.V. Rotkin, and N. R. Aluru, *Nanotechnology* **13**, 120 (2002).
- 17 C.-H. Ke, B. Peng, N. Pugno, and H. D. Espinosa "Experiments and modeling of carbon-nanotube based NEMS devices," submitted to *Journal of Mechanics and Physics of Solids*, 2004.
- 18 R. Tarkiainen, M. Ahlskog, J. Penttila, L. Roschier, P. Hakonen, M. Paalanen, and E. Sonin, *Phys. Rev. B* (**64**), 195412
- 19 J. Sun, Z. X. Zhang, S. M. Hou, G. M. Zhang, Z. N. Gu, X. Y. Zhao, W. M. Liu, and Z. Q. Zue, *Appl. Phys. A* **75**, 479 (2002).
- 20 P. A. Williams, S. J. Papadakis, and M. R. Falvo, *Appl. Phys. Lett.* **80**, 2574 (2002).
- 21 M. F. Yu, O. Lourie, M. J. Dyer, K. Moloni, T. F. Kelly, and R. S. Ruoff, *Science* **287**, 637 (2000).
- 22 Y. G. Zhang, A. Chang, J. Cao, Q. Wang, W. Kim, Y. M. Li, N. Morris, E. Yenilmez, J. Kong, and H. J. Dai, *Appl. Phys. Lett.* **79**, 3155 (2001).
- 23 K. Yamamoto, S. Akita, and Y. Nakayama, *J. Phys. D* **31**, L34 (1998).
- 24 A. Bezryadin and C. Dekker, *Appl. Phys. Lett.* **71**, 1273 (1997).
- 25 D. G. Fertis, *Nonlinear Mechanics*, CRC Press, 1999, 2nd Edition.
- 26 M. M. J. Treacy, T. W. Ebbesen, and J. M. Gibson, *Nature* **381**, 678 (1996).

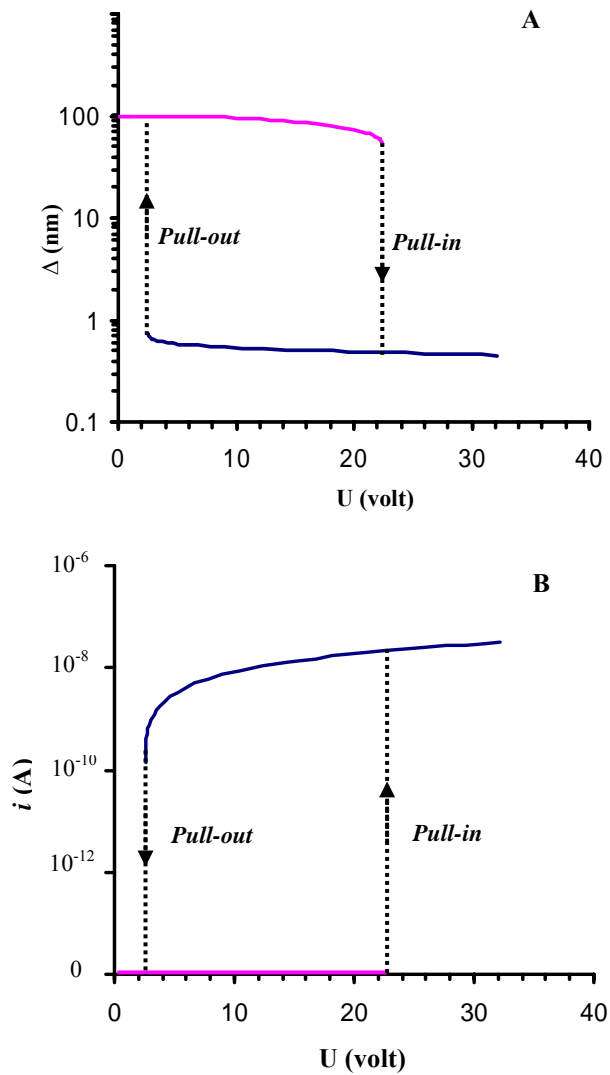


Figure 3. Characteristic of *pull-in* and *pull-out* processes for a device with $R_{\text{ext}}=9.015$ nm, $R_{\text{int}}=6$ nm, $L=500$ nm, $H = 100$ nm, $R_o=1$ K Ω and $R = 1$ G Ω . (A) shows the relation between the gap Δ and the applied voltage U . (B) shows the relation between the current i in the circuit and the applied voltage U .

In summary, in this paper, an innovative feedback-controlled switchable CNT-based NEMS device is proposed. Although the discussion is based on CNT cantilevers, other possibilities include doped Si nanowires and other materials, which could be more easily integrated to current microelectronics technology. The electrical-mechanical characteristics of the device were examined, and some key issues in its design were highlighted. Future work would focus on the micro/nanofabrication of the device and its dynamic analysis. Potential applications for the device include: NEMS switches, nonvolatile random access memory elements, electron counters, logic devices and gap sensing devices.